

# Cyclic voltammetric analysis of C<sub>1</sub>–C<sub>4</sub> alcohol electrooxidations with Pt/C and Pt–Ru/C microporous electrodes

Choong-Gon Lee<sup>a,\*</sup>, Minoru Umeda<sup>b</sup>, Isamu Uchida<sup>c</sup>

<sup>a</sup> Department of Chemical Engineering, Hanbat National University, San 16-1 Dukmyung-dong, Yusong-gu, Daejeon, Korea

<sup>b</sup> Department of Chemistry, Nagaoka University of Technology, Kamitomioka, Nagaoka, Japan

<sup>c</sup> Department of Applied Chemistry, Tohoku University, Aramaki-aoba, Aoba-ku, Sendai, Japan

Received 3 August 2005; accepted 12 January 2006

Available online 2 March 2006

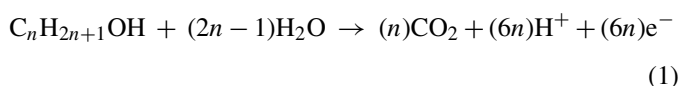
## Abstract

The effect of temperature on methanol, ethanol, 2-propanol, and 2-butanol electrooxidation is investigated with Pt/C and Pt–Ru/C microporous electrodes. Cyclic voltammetry is employed in temperatures ranging from 25 to 80 °C to provide quantitative and qualitative information on the kinetics of alcohol oxidation. Methanol displays the greatest activity among alcohols. The addition of ruthenium reduces the poisoning effect, although it is ineffective with secondary alcohols. Secondary alcohols undergo a different oxidation mechanism at higher temperatures. Microporous electrodes provide detailed information on alcohol oxidation.

© 2006 Elsevier B.V. All rights reserved.

## 1. Introduction

A direct alcohol fuel cell (DAFC) that uses hydrocarbon liquid fuel has several merits, namely it has a high specific energy, does not require a reformer, and it is easy to handle the liquid alcohol fuel. Methanol, ethanol, propanol and butanol have all been considered as alcohol fuels. The general equation for alcohol oxidation may be written as:



Considerable research has focused on methanol electrooxidation. Formic acid and formaldehyde are formed as intermediate species during progress to the final product of carbon dioxide [1–3]. Methanol has been considered as the most appropriate fuel for the DAFC. On the other hand, ethanol has much less toxicity and also has a higher specific energy. Consequently, ethanol electrooxidation can be considered to be an important research topic. It has been reported [4] that ethanol is oxidized to acetaldehyde and CO<sub>2</sub> by a dual-path mechanism in which oxidation to CO<sub>2</sub> proceeds via adsorbed intermediates and to acetaldehyde by the dehydrogenation of adsorbed ethanol [4].

Acetic acid formation during ethanol oxidation has been found to depend on the applied potential. Acetaldehyde is dominant at a potential under 0.6 V versus RHE, whereas acetic acid is dominant above 0.8 V versus RHE [5].

Recent studies [6,7] have focused on 2-propanol as an alcohol fuel because it shows a lower overpotential and higher performance than methanol. Alcohols with more than two carbon atoms have several isomers, and special features of non-CO adsorptions at 2-propanol have been reported [8]. It has also been found that C–C cleavage in secondary alcohols is difficult as the electronic effect depends on the position at which OH is adsorbed on the carbon atom [8–11]. Another difference between normal and isomeric alcohols is that 1-propanol produces propanal, propionic acid and CO<sub>2</sub>, while 2-propanol produces acetone and CO<sub>2</sub> with a less poisoning effect [8]. In this context, 2-butanol shows non-CO production and has less reactivity than the 1-butanol with a different reaction mechanism, and tertiary butanol is almost totally unreactive [12,13].

To date, Pt has been recognized as the most active electrocatalyst for alcohol oxidation. There is a drawback, however, in that Pt is easily poisoned by the reaction intermediate, CO. Adding Ru to Pt is an effective way to reduce the effect of poisoning through a bifunctional mechanism [14] in which Ru adsorbs H<sub>2</sub>O, the form Ru–OH, at a lower potential than Pt and supplies oxygen species to oxidize adsorbed CO on Pt to CO<sub>2</sub>. This mechanism adequately accounts for methanol oxidation on

\* Corresponding author. Tel.: +82 42 821 1529; fax: +82 42 821 1593.  
E-mail address: [leecg@hanbat.ac.kr](mailto:leecg@hanbat.ac.kr) (C.-G. Lee).

Pt–Ru. For ethanol oxidation, it has been reported [4,15,16] that Pt–Ru shows less current density than Pt due to the inactivity of Ru. The effect of Ru addition on propanol oxidation appears insignificant, although 1-propanol displays a lower onset potential [8].

In terms of the effect of temperature, it is clear that the rates of methanol and ethanol oxidation increase at higher temperatures. In particular, Ru oxidizes methanol at above 70 °C, while it is inactive below this temperature [17,18]. Unusual behaviour has been reported for 2-butanol in that the activation energy becomes zero or negative over 45 °C, whereas 1-butanol and isobutanol have positive activation energies [9].

In previous work [19], the temperature effect of methanol and ethanol electrooxidation was investigated with Pt/C and Pt–Ru/C microporous electrodes that could exclude the effects of the polymeric binder that was used to fabricate electrodes with a porous type of material. Differences were clearly observed between Pt/C and Pt–Ru/C for methanol and ethanol oxidations; methanol and ethanol gave different cyclic voltammograms and the addition of Ru resulted in a higher increase in current with increase in temperature because of the bifunctional effect with both alcohols.

In this work, cyclic voltammetry is used to investigate the temperature effect on alcohol oxidation in C<sub>1</sub> to C<sub>4</sub> alcohols. Carbon-supported Pt and Pt–Ru are used in microporous electrodes at temperatures between 25 and 80 °C.

## 2. Experimental

The alcohols used in this work were methanol, ethanol, 2-propanol and 2-butanol. Each of the four alcohol solutions was prepared by mixing 0.5 M of the alcohol with 0.5 M of H<sub>2</sub>SO<sub>4</sub> solution.

The electrocatalysts were carbon-supported Pt (Pt/C) and Pt–Ru (Pt–Ru/C) supplied by Tanaka Kikinzo Co. The platinum content of Pt/C was 45.9 wt.%, while Pt–Ru/C was composed of 29.8 wt.% Pt and 23.1 wt.% Ru (atomic ratio of Pt/Ru = 2/3). All were used as-received.

A microporous electrode filled with electrocatalysts in a cylindrical pore 50 μm in diameter and 10 μm in depth served as the working electrode. A gold lead wire was used for the microporous electrode. The reference electrode was Ag|AgCl, and Pt black served as the counter electrode. Unless otherwise stated, all potentials are expressed with respect to the reversible hydrogen electrode (RHE). To investigate the effect of temperature on alcohol oxidation, a gas-tight electrochemical cell was employed. More details are given elsewhere [19]. The cell temperature was controlled to between 25 and 80 °C in a forced convection oven.

Electrochemical measurements were mainly conducted with cyclic voltammetry (CV). A low current potentiostat (Hokutodenko, HAB-150) and a function generator (Hokutodenko, HAB-151) were employed. Prior to CV measurement, the alcohol solutions were de-aerated by nitrogen bubbling and the electrocatalysts were activated by conducting 10 cycles between –0.1 and 1.0 V versus Ag|AgCl.

## 3. Results and discussion

### 3.1. Alcohol oxidation at Pt/C

#### 3.1.1. Effect of temperature on alcohol oxidation

Fig. 1(a)–(d) show cyclic voltammograms (CVs) at different temperatures for the methanol, ethanol, 2-propanol, and 2-butanol solutions, respectively. Methanol is the lightest alcohol, thus its reaction processes are relatively smooth with few reaction intermediates such as formic acid, formaldehyde, and CO. Methanol gives an oxidation peak (a<sub>1</sub>) on the positive potential scan and a re-oxidation peak on the negative potential scan, as shown in Fig. 1(a). Platinum is the most active electrocatalyst. Methanol is adsorbed on the Pt surface and is oxidized to CO through a dehydrogenation process. Further oxidation of CO requires oxygen species from water. It has been reported [20] that water adsorption on Pt commences at 0.7 V. The onset potential of the methanol oxidation peak occurs at about 0.6 V in this work (Fig. 1(a)). At potentials above 0.9 V, an oxide species from water decomposition covers the Pt surface and leads to a decrease in oxidation current. A reduction of the oxide species on the negative potential scan allows re-oxidation of the intermediate species. With increasing temperature, a negative shift in the onset potential and larger oxidation currents are observed. In addition, a negative shift in the oxidation peak and a positive shift in the re-oxidation peak are also observed. This trend is caused by higher temperatures facilitating the adsorption of water on to Pt and the desorption of oxide species from Pt. A vertical increase in the re-oxidation current at 80 °C supports this assumption.

Ethanol exhibits rather complex oxidation processes, as indicated in Fig. 1(b). Compared with methanol oxidation (Fig. 1(a)), lower onset potentials are observed. Assuming that water adsorption on Pt takes place at about 0.6 V, based on the methanol oxidation in Fig. 1(a), the lower onset potential of about 0.4 V indicates that dehydrogenation of ethanol occurs until water adsorption commences [8]. Two oxidation peaks, at about 0.9 V (a<sub>1</sub>) and 1.3 V (a<sub>2</sub>), are observed on the positive potential scan and multiple re-oxidation peaks appear on the negative potential scan. From a differential electrochemical mass spectrometry (DEMS) study, Fujiwara et al. [16] suggested that the oxidation peak 'a<sub>1</sub>' is ascribed to CO<sub>2</sub> production and that acetaldehyde formation leads to peak 'a<sub>2</sub>'. On the other hand, Hitmi et al. [5] reported that ethanol oxidizes to acetaldehyde at a lower potential (<0.6 V) and to acetic acid at a higher potential (>0.8 V), whereas the DEMS analysis by Schmidt et al. [4] suggested that acetic acid does not form at all during ethanol oxidation. With increasing temperature, the onset potential for ethanol oxidation shifts in a negative direction. On the other hand, the potentials of the 'a<sub>1</sub>' and 'a<sub>2</sub>' peaks do not shift negatively, which is converse behaviour to that of methanol oxidation as shown in Fig. 1(a). By contrast, the peak potentials for ethanol shift positively with a broadening of the peak width. If we assume that the negative shift of peak potential for methanol oxidation is due to increased adsorption of OH adsorption, which is caused by water decomposition at high temperatures, then the positive potential shift and peak broadening for ethanol oxidation would

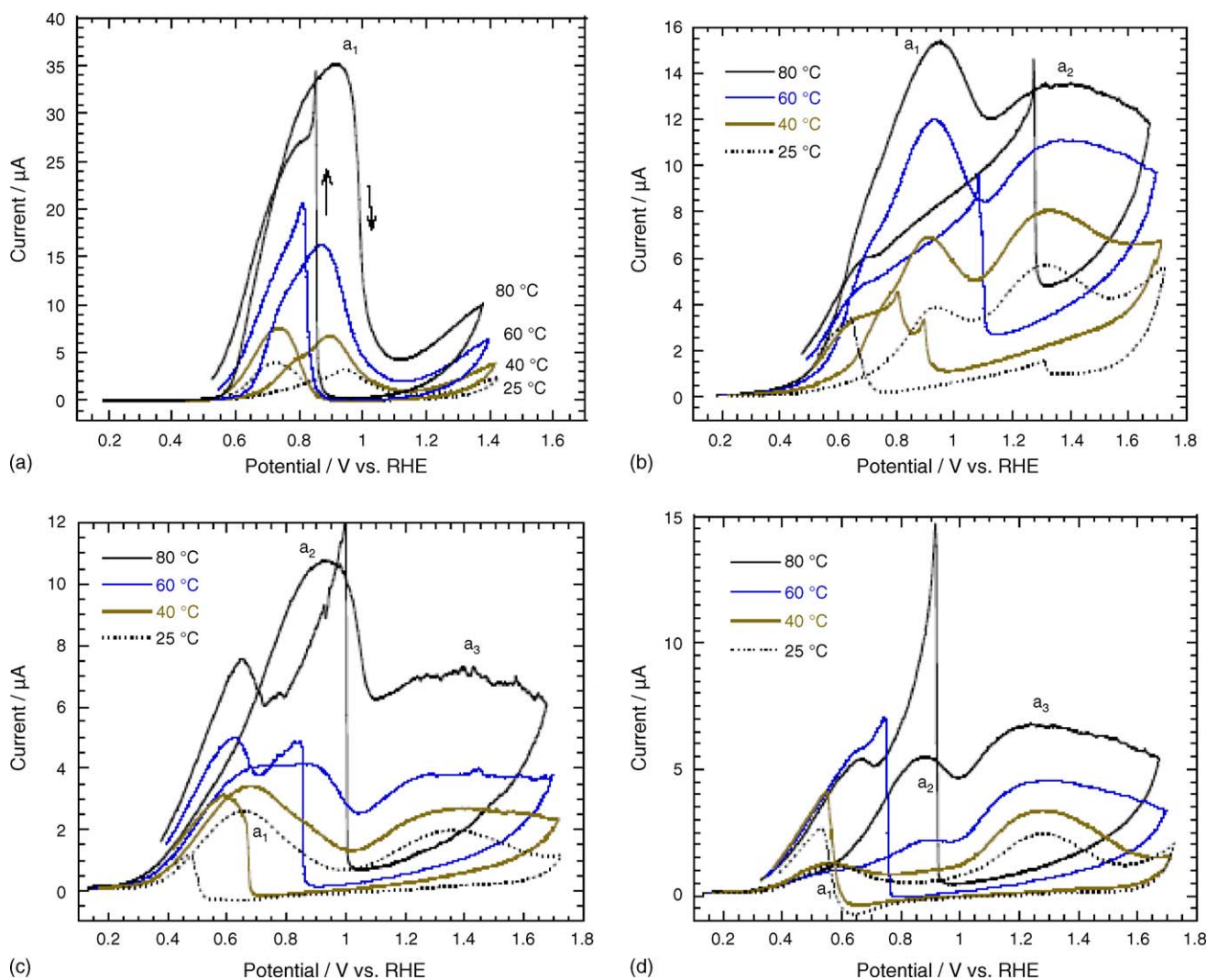


Fig. 1. Cyclic voltammograms at different temperatures with Pt/C in (a) 0.5 M methanol + 0.5 M H<sub>2</sub>SO<sub>4</sub>, (b) 0.5 M ethanol + 0.5 M H<sub>2</sub>SO<sub>4</sub>, (c) 0.5 M 2-propanol + 0.5 M H<sub>2</sub>SO<sub>4</sub>, (d) 0.5 M 2-butanol + 0.5 M H<sub>2</sub>SO<sub>4</sub>. Scan rate = 0.1 V s<sup>-1</sup>.

suggest that the currents of the 'a<sub>1</sub>' and 'a<sub>2</sub>' peaks are independent of OH adsorption. This probably results in the observed lower temperature dependence of the peak currents for ethanol. On the other hand, a distinct positive shift of the re-oxidation peaks is observed with increase in temperature. Compared with methanol oxidation, the potential shift in ethanol is significant. Ethanol produces more reaction intermediates than methanol, so the Pt surface will be significantly covered with intermediate species. Thus, it can be concluded that ethanol gives weak OH adsorptivity on Pt and that it is readily desorbed with increase in temperature. The vertical increase of the re-oxidation current at higher temperatures supports this assumption. The multiple re-oxidation peaks also indicate the complexity of the adsorbed reaction intermediates.

2-Propanol exhibits an even more complicated oxidation behaviour (Fig. 1(c)). A very low onset potential at about 0.3 V is observed. Oxidation of 2-propanol involves 18 electron transfers, thus the process is very complicated. Considering that the OH adsorption by water decomposition on the Pt surface occurs at about 0.6 V, the low onset potential is probably due to dehy-

drogenation of 2-propanol. Although 2-propanol shows a very low onset potential, the value does not exhibit a clear dependence on the temperature. The complexity of the oxidation process can be a reason for this, and the independence of the onset potential on temperature reflects the low activity of 2-propanol.

For 2-propanol oxidation, three oxidation peaks are observed at about 0.65 V (a<sub>1</sub>), 0.9 V (a<sub>2</sub>), and 1.3 V (a<sub>3</sub>), as shown in Fig. 1(c). Looking carefully at methanol and ethanol oxidation, current shoulders on the positive potential scan can be observed at about 0.8 V for methanol oxidation (Fig. 1(a)) and at 0.7 V for ethanol oxidation (Fig. 1(b)), although the reasons for these remain unclear. The CV for 2-propanol oxidation at 80 °C (Fig. 1(c)) resembles the CV for ethanol oxidation at 80 °C (Fig. 1(b)). In this connection, the oxidation of 'a<sub>1</sub>' would arise for the same reason as the current shoulders seen above for methanol and ethanol. With decreasing temperature, the 'a<sub>2</sub>' peak diminishes and finally disappears at 25 °C. Only two peaks, 'a<sub>1</sub>' and 'a<sub>3</sub>', are observed at 25 °C. This temperature behaviour indicates that the reaction paths of 2-propanol differ with varying temperature. At higher temperatures, the oxidation is similar to

ethanol oxidation, but it follows a different reaction mechanism at lower temperatures. Multiple re-oxidation peaks with a vertical increase are observed, which indicates multiple oxidations of the adsorbed reaction species and a weak OH adsorptivity on the Pt surface.

The effects of temperature on the oxidation of 2-butanol are more obvious, as seen in Fig. 1(d). Three oxidation peaks, 0.55 V ( $a_1$ ), 0.9 V ( $a_2$ ) and 1.3 V ( $a_3$ ) are observed. Only the ' $a_2$ ' and ' $a_3$ ' peaks are observed at 80 °C while ' $a_1$ ' and ' $a_3$ ' are observed at 25 °C. This behaviour is very similar to that shown by 2-propanol oxidation for which the reaction mechanism depends on the temperature. In particular, the peak current of ' $a_1$ ' decreases with temperature. This indicates that ' $a_1$ ' is dominant at lower temperatures, while ' $a_2$ ' prevails at higher temperatures. This is in line with the report of Takky et al. [9] that the activation energy of 2-butanol oxidation over 45 °C is either zero or negative and the mechanism undergoes a change. Very large re-oxidation peaks are also observed. With increasing carbon chain from methanol to 2-butanol, the re-oxidation peaks become larger. Since a re-oxidation peak represents the oxidation of a surface-adsorbed species, a higher carbon-chain alcohol results in a significant amount of surface adsorption species. In addition, reduction currents of adsorbed oxide species are observed at around 0.6 V at 25 °C, which indicates that a strong adsorption of oxide on the Pt surface takes place at lower temperatures.

### 3.2. Effect of scan rate variation

Fig. 2(a) and (b) show CVs of methanol oxidation at 25 and 80 °C, respectively. At 25 °C, peak currents increase with the scan rate. In principle, peak currents are proportional to the scan rate at the adsorption process and have 0.5 orders to scan rate at diffusion process [21]. Currents at about 0.65 V increase with scan rate, while the current shoulder at 0.8 V diminishes. Thus, a lower onset potential is observed at a higher scan rate. As mentioned above, in Section 1.1, methanol oxidation commences by

the oxidative adsorption of water on the Pt surface at around 0.6 V and the currents at 0.65 V increase with scan rate. Thus, it can be assumed that the water adsorption process is related to the oxidation process at 0.65 V. This assumption allows for the fact that the oxidative adsorption of water starts at a lower potential with increasing scan rates. In addition, the current shoulder at 0.8 V is reduced with increasing scan rates. Thus, it can be concluded that the oxidation process at 0.65 V is related to the process at the current shoulder at 0.8 V.

The dependence of the peak potential on the scan rate also provides kinetic information. A peak potential which is independent of the scan rate indicates a reversible charge-transport process, whereas an irreversible charge-transfer process causes the peak potential to vary with scan rate [21]. A relationship between the oxidation and re-oxidation peak potentials is observed, which indicates that methanol oxidation at low temperatures is an irreversible charge-transfer process.

A clear dependence of peak potential and peak currents on the scan rate is not, however, observed at 80 °C, as shown in Fig. 2(b). Although the peak potential on the positive scan varies slightly with scan rate, methanol oxidation appears to be very facile at 80 °C. The fact that the current and the potential of the re-oxidation peak are not dependent on scan rate support this assumption. The overlapping of the oxidation and re-oxidation peaks also suggest a very fast reaction kinetics. The larger onset potential at the higher scan rate, contrary to Fig. 2(a), cannot, however, be explained at this stage.

Fig. 3(a) and (b) display the CV results for ethanol oxidation at 25 and 80 °C, respectively. It is found that the current shoulder at about 0.7 V diminishes with increasing scan rate at 25 °C and that the current rises at around 0.55 V in the case of a 0.1 V s<sup>-1</sup> scan rate. This is similar to what was observed in the case of the methanol oxidation in Fig. 2(a). The peak potentials of the ' $a_1$ ' and ' $a_2$ ' peaks show a slight dependence on scan rate at 25 °C, which indicates some irreversibility in the charge-transfer process. On the other hand, the peak cur-

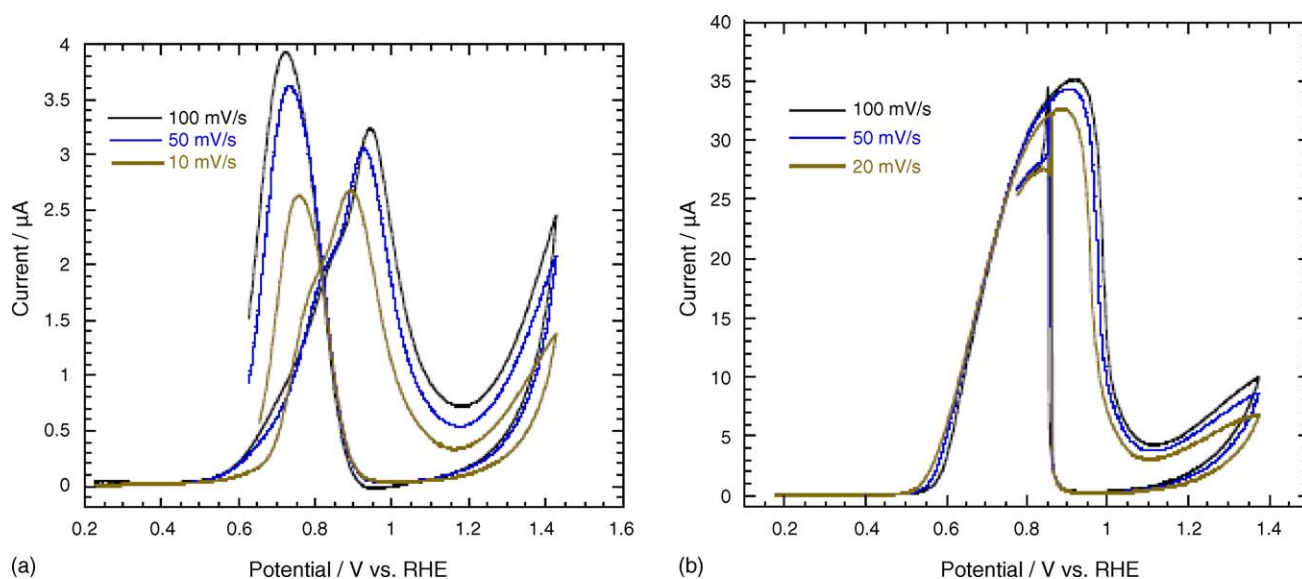


Fig. 2. Cyclic voltammograms at different scan rates with Pt/C in 0.5 M methanol + 0.5 M H<sub>2</sub>SO<sub>4</sub>, at (a) 25 °C and (b) 80 °C.



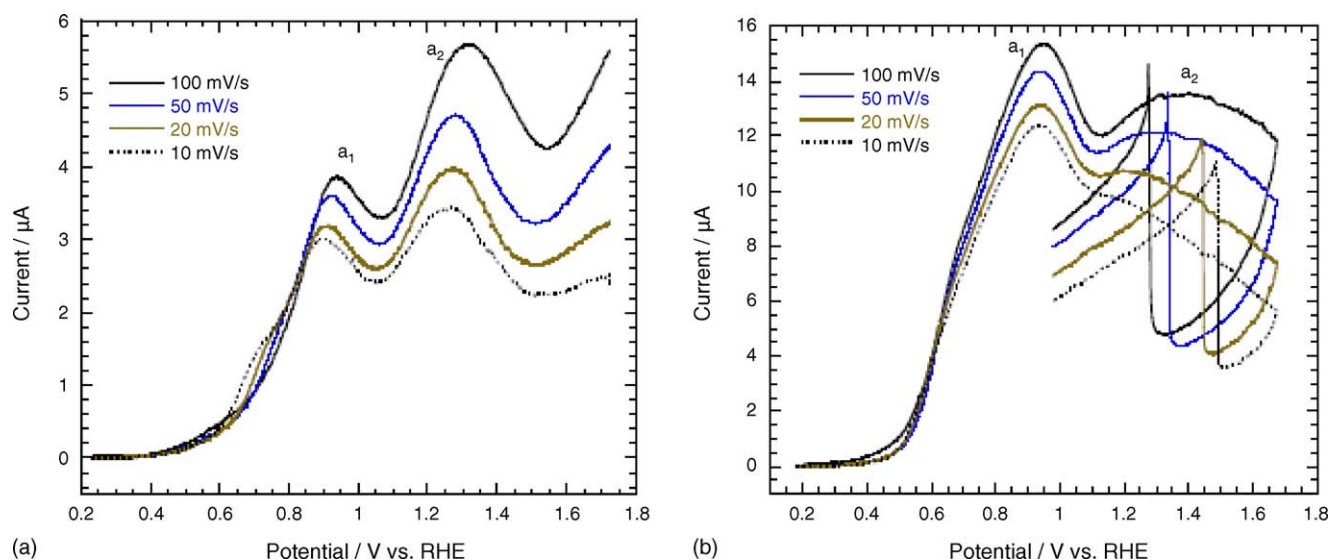
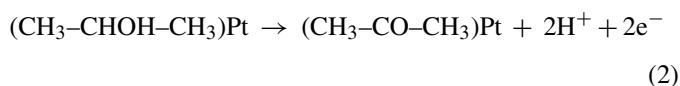


Fig. 3. Cyclic voltammograms at different scan rates with Pt/C in 0.5 M ethanol + 0.5 M H<sub>2</sub>SO<sub>4</sub>, at (a) 25 °C and (b) 80 °C.

rents of 'a<sub>1</sub>' show less dependence on scan rate than those of 'a<sub>2</sub>', which suggests that adsorption is more significant at the oxidation process of 'a<sub>2</sub>' around 1.3 V. The peak potential of 'a<sub>1</sub>' is independent of the scan rate at 80 °C, as shown in Fig. 3(b). This indicates that ethanol oxidation at 80 °C is a very fast reaction. In Fig. 3(b), which shows the scan rate dependence of currents, the broad peaks at around 1.4 V indicate an adsorption prevailing processes. These adsorption processes probably result in the scan rate dependence of the re-oxidation potentials.

Fig. 4(a)–(d) give the CV results for 2-propanol oxidation at 25, 40, 60, and 80 °C, respectively. Fig. 4(a) contains two distinct current peaks, at about 0.65 V (a<sub>1</sub>) and 1.35 V (a<sub>3</sub>), with a small current peak at about 0.9 V (a<sub>2</sub>). Even at a low temperature of 25 °C, the potentials of 'a<sub>1</sub>' and 'a<sub>3</sub>' do not depend on the scan rate, and this means that these reactions are very fast and include a reversible charge-transfer process. The fast reaction of 2-propanol can be explained by comparing 2-propanol oxidation with methanol oxidation. The lightest alcohol, methanol, experiences a shift in peak potential with scan rate, as shown in Fig. 2(a), and previous work [22] has demonstrated that oxidation and re-oxidation peaks correspond to oxidation of methanol to the final product, CO<sub>2</sub>, via CO adsorption. On the other hand, the oxidation and re-oxidation peaks of 2-propanol are caused by acetone production and, furthermore, 2-propanol does not produce CO adsorbates because C–C bonds do not break on Pt [8,10]. Therefore, the oxidation of 2-propanol produces only two electrons per molecule, i.e.,



Compared with the 6-electron transfer for methanol oxidation to CO<sub>2</sub>, oxidation of 2-propanol to the acetone of Eq. (2) is more facile. When the temperature is increased to 40 °C, the 'a<sub>2</sub>' peak becomes dominant without dependence on the scan rate. Thus, an oxidation process at about 0.9 V and independent

of the scan rate could be considered quite fast. The 'a<sub>2</sub>' peak is more dominant at 60 °C, as shown in Fig. 4(c). The 'a<sub>1</sub>' peak becomes relatively small, compared with the 'a<sub>2</sub>' peak, and is only observed with a 0.1 V s<sup>-1</sup> scan rate. At 80 °C, the 'a<sub>1</sub>' peak transforms into a current shoulder at about 0.5 V and the 'a<sub>2</sub>' peak is dominant in the oxidation process, as shown in Fig. 4(d).

2-Butanol oxidation has similarities with 2-propanol oxidation, as illustrated by Fig. 5(a) and (b). Two dominant current peaks, at about 0.55 V (a<sub>1</sub>) and 1.3 V (a<sub>3</sub>), are observed in Fig. 5(a), with a very small peak at about 0.9 V (a<sub>2</sub>). The peak potentials of the 'a<sub>1</sub>' peak and the 'a<sub>3</sub>' peak are both independent of scan rate at 25 °C. As mentioned above, the invariance of the peak potential for the 2-propanol oxidation, represents the presence of a reversible charge-transfer process. In addition, 2-butanol is much less poisonous among the butanol isomers [9,13]. It is concluded that the oxidation of 2-butanol is similar to that of 2-propanol oxidation as shown by Eq. (2). At 80 °C, the 'a<sub>1</sub>' peak diminishes to a current shoulder and the 'a<sub>2</sub>' peak is almost independent of the scan rate. The 'a<sub>3</sub>' peak is the dominant process in 2-butanol oxidation.

Table 1 summarizes the kinetic values of the onset potential, peak potentials, peak currents, logarithmic ratio of peak current to scan rate  $\log(i)/\log(v)$ , and activation energies for methanol, ethanol, 2-propanol and 2-butanol oxidations. The onset potential of alcohol oxidation becomes negative with increasing carbon number. 2-propanol shows the most negative onset potentials, probably due to its very low dehydrogenation potentials. Methanol displays the highest current increase with temperature. Temperature effects appear insignificant for the secondary alcohols, although 2-propanol exhibits a relatively large current increase with a different oxidation mechanism at a higher temperature. Except for the 'a<sub>1</sub>' peaks of the secondary alcohols, the slopes of  $\log(i)/\log(v)$  are much less than 0.5, which indicates that these oxidation processes are diffusion-controlled. By contrast, the 'a<sub>1</sub>' peaks for 2-butanol have a slope of about 0.8, which suggests that adsorption is dominant for the process. In particular, the 'a<sub>2</sub>' peaks for the secondary alcohols show very

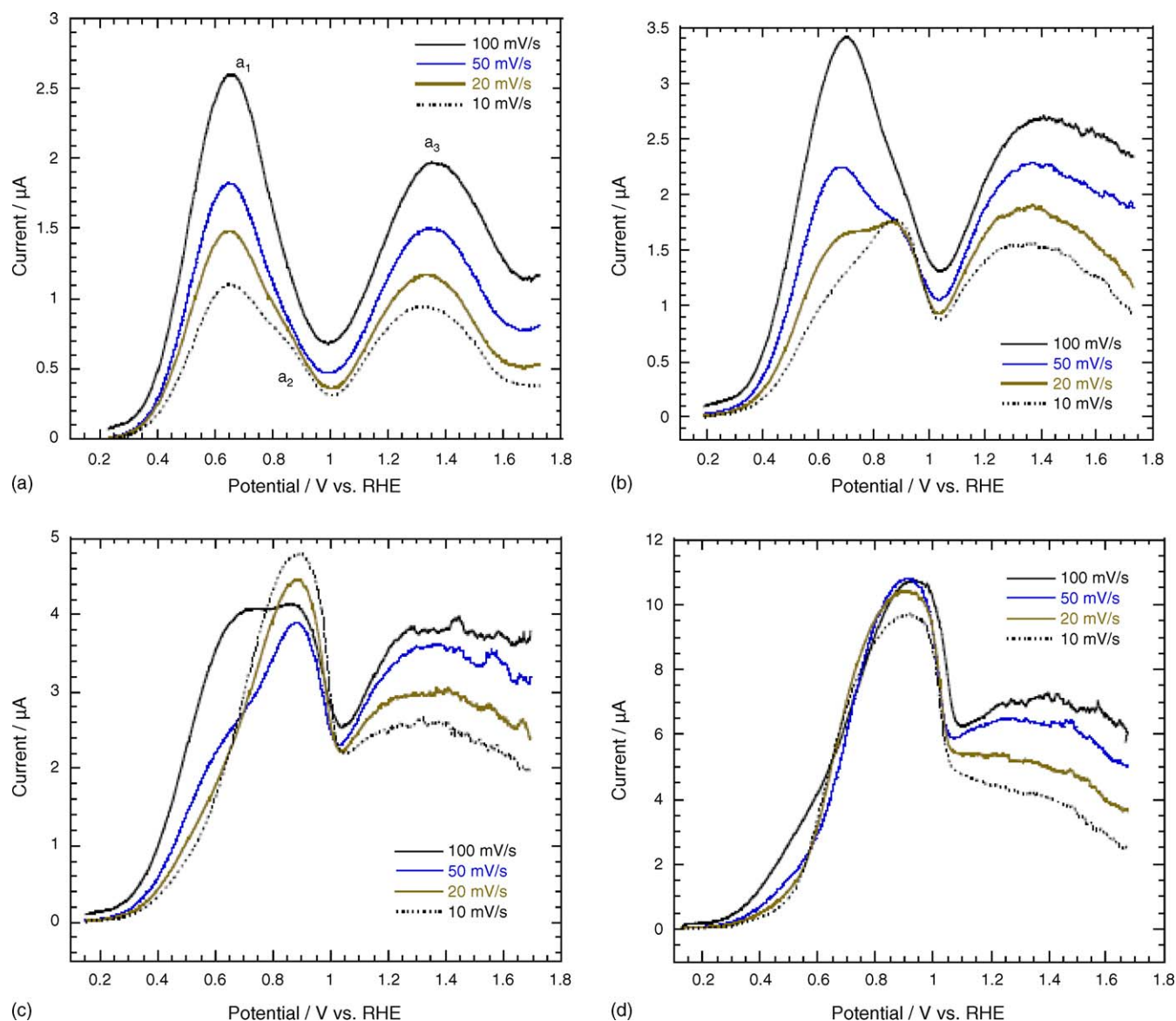


Fig. 4. Cyclic voltammograms at different scan rates with Pt/C in 0.5 M 2-propanol + 0.5 M H<sub>2</sub>SO<sub>4</sub>, at (a) 25 °C, (b) 40 °C, (c) 60 °C, (d) 80 °C.

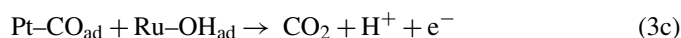
low  $\log(i)/\log(v)$  values at higher temperatures. In addition, the activation energies of these peaks are very close to those of methanol oxidation. Thus process similar to that of methanol oxidation probably occurs during the oxidation of secondary alcohol at high temperatures.

#### 4. Alcohol oxidations at Pt–Ru/C

##### 4.1. Temperature effect on alcohol oxidations

Fig. 6(a)–(d) show methanol, ethanol, 2-propanol and 2-butanol oxidation behaviour, respectively, at a Pt–Ru/C microporous electrode. It should be noted that Ru is unstable above 0.9 V because it is oxidized. Nevertheless, cycling up to 1.3 V gives reproducible CVs. At this stage, the oxidation effect of Ru cannot be explained; further investigations are required. Fig. 6(a) presents CVs for methanol oxidation at temperatures ranging from 25 to 80 °C. The effect of adding Ru on the

methanol oxidation is explained by the following bifunctional mechanism.



Methanol is adsorbed on the Pt surface and is oxidized to CO. Although Ru has been reported as inactive for the methanol oxidation [23], Ru oxidatively decomposes water and OH is strongly adsorbed on the Ru surface. Thus, Ru supplies oxygen species for CO oxidation and promotes methanol oxidation. The OH adsorption on the Ru surface commences at 0.2 V [20], which shifts the onset potential of methanol oxidation negatively. This behavior is confirmed by the comparison of Pt–Ru/C in Fig. 6(a) with Pt/C in Fig. 2(a). A negative shift of about 100 mV is observed at Pt–Ru/C. This strong adsorption of OH

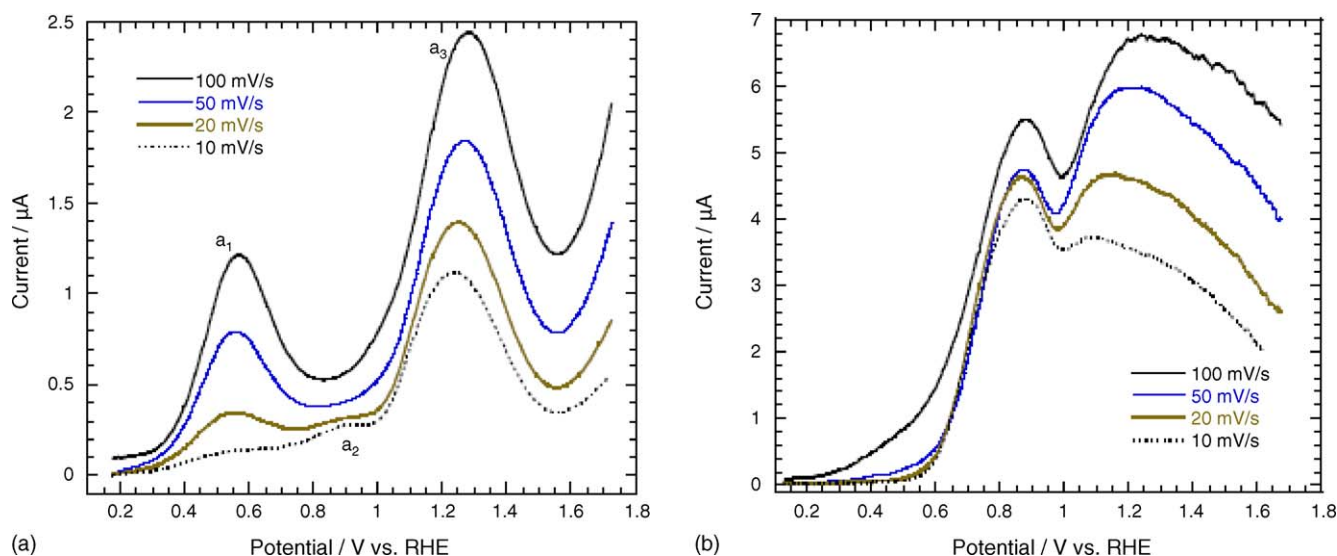


Fig. 5. Cyclic voltammograms at different scan rates with Pt/C in 0.5 M 2-butanol + 0.5 M H<sub>2</sub>SO<sub>4</sub>, at (a) 25 °C, and (b) 80 °C.

on Ru results in a mild current increase in the re-oxidation peaks. The smaller re-oxidation peaks also suggest that Ru reduces the effects of poisoning in methanol oxidation. At higher temperatures, the oxidation and re-oxidation peak potentials are quite close. The reason for this is that OH adsorbs on Ru at a lower potential with increasing temperature, while adsorbed OH is readily desorbed at higher temperatures.

The effect of adding Ru on ethanol oxidation remains inconclusive. Nevertheless, much research has suggested that Ru addition reduces the rate of ethanol oxidation because Ru is inactive for this reaction and because the number of active Pt sites is reduced by the presence of Ru [4,15,16]. On the other hand, it has also been reported [15] that Ru promotes dehydrogenation and facilitates C–C bond breaking; thus, CO<sub>2</sub> selectivity is increased

with increased amounts of Ru. Fig. 6(b) shows the effect of temperature on ethanol oxidation on Pt–Ru/C. Unlike the results obtained with Pt/C in Fig. 1(b), the peak current on the positive scan much increases with temperature. Current increases of about 8 times are observed with Pt–Ru/C, while Pt/C showed an increase of only about 4 times over the same temperature range. Another difference is that the potentials of the oxidation and the re-oxidation peaks become closer at higher temperatures. This potential shift is not observed for ethanol oxidations with Pt/C in Fig. 2(b). If it is assumed that the product in the potential range is CO<sub>2</sub> as according to Fujiwara et al. [16], then it is possible that the ethanol adsorbed on the Pt site is oxidized to CO by the synergistic effect of Ru. In fact, it has been reported [15] that Ru promotes dehydrogenation and facilitates rupture of the C–C

Table 1  
Kinetic values of various alcohol oxidations with Pt/C microporous electrode

Alcohols	Temperature (°C)	Onset potential (V vs. RHE)	Peak potential, $E_p$ (V at 0.1 V s <sup>-1</sup> )			Peak current, $I_p$ (µA at 0.1 V s <sup>-1</sup> )			Slope of $\log(i)/\log(v)^a$			Activation Energy/kJ mol <sup>-1</sup>		
			a <sub>1</sub>	a <sub>2</sub>	a <sub>3</sub>	a <sub>1</sub>	a <sub>2</sub>	a <sub>3</sub>	a <sub>1</sub>	a <sub>2</sub>	a <sub>3</sub>	a <sub>1</sub>	a <sub>2</sub>	a <sub>3</sub>
Methanol	25	0.645	0.945			3.23			0.08			37.7		
	40	0.615	0.895			6.76			0.05					
	60	0.595	0.865			16.27			0.04					
	80	0.545	0.915			35.10			0.07					
Ethanol	25	0.501	0.933	1.315		3.85	5.65		0.11	0.21		22.1	13.9	
	40	0.427	0.912	1.325		6.88	8.03		0.14	0.22				
	60	0.378	0.928	1.375		11.97	11.12		0.20	0.22				
	80	0.351	0.943	1.395		15.37	13.54		0.09	0.14				
2-Propanol	25	0.317	0.654			2.61			0.36		0.31	10.4	37.6	15.6
	40	0.247	0.700	0.902	1.352	3.40	2.08	1.97	0.45	0.06	0.23			
	60	0.226	0.715	0.890	1.381	4.07	4.79	2.68	0.90	0.09	0.18			
	80	0.202		0.936	1.375		10.73	3.82		0.04				
2-Butanol	25	0.315	0.569		1.279	1.22		2.44	0.78		0.32	2.1	44.8	15.8
	40	0.305	0.563		1.375	1.27		3.35			0.30			
	60	0.244		0.901	1.292		2.19	4.53		0.06	0.22			
	80	0.221		0.880	1.255		5.48	6.74		0.09	0.26			

<sup>a</sup>  $v$ : scan rate.

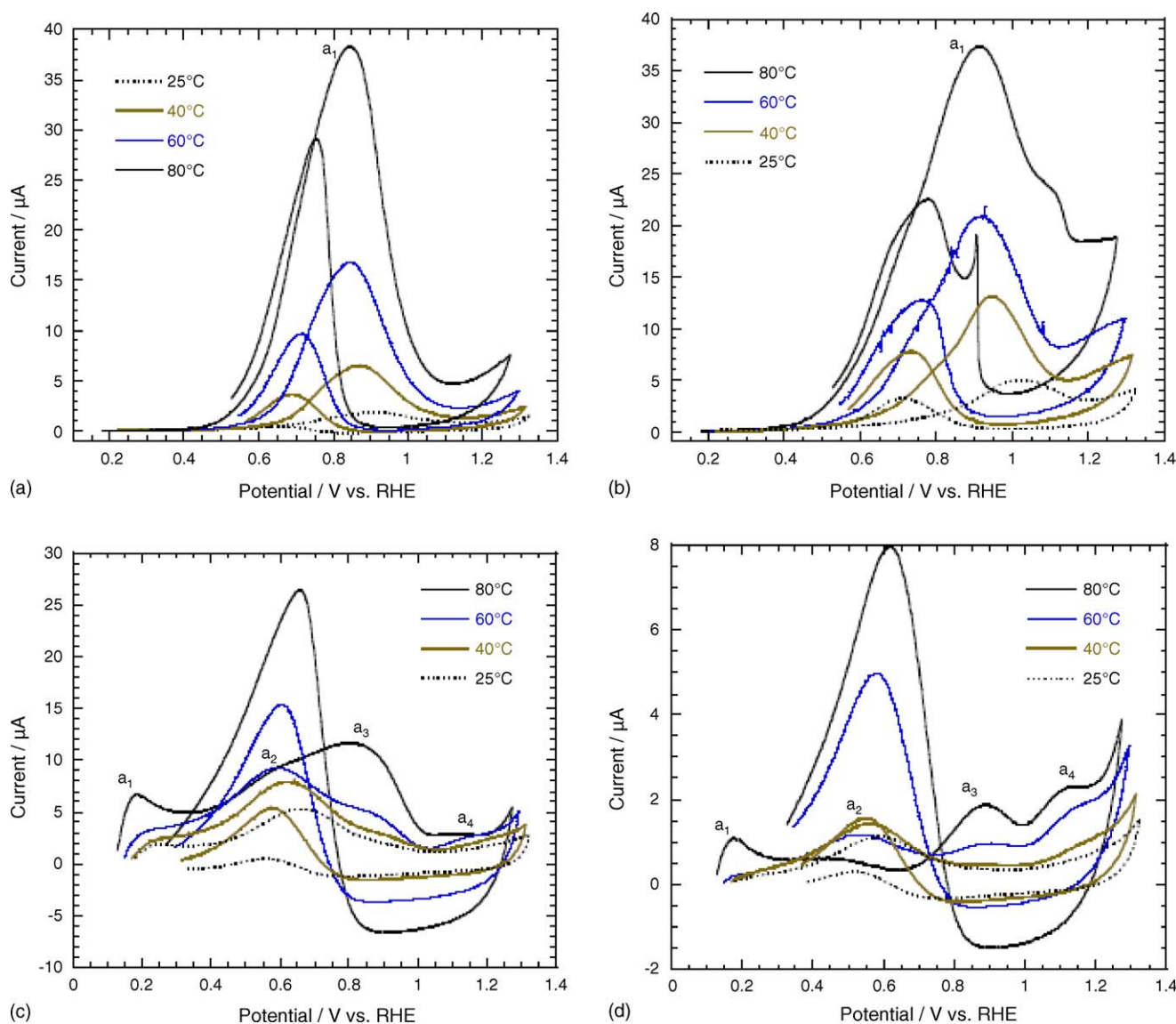


Fig. 6. Cyclic voltammograms at different temperatures with Pt-Ru/C in (a) 0.5 M methanol + 0.5 M H<sub>2</sub>SO<sub>4</sub>, (b) 0.5 M ethanol + 0.5 M H<sub>2</sub>SO<sub>4</sub>, (c) 0.5 M 2-propanol + 0.5 M H<sub>2</sub>SO<sub>4</sub>, (d) 0.5 M 2-butanol + 0.5 M H<sub>2</sub>SO<sub>4</sub>. Scan rate = 0.1 V s<sup>-1</sup>.

bond. If so, then Ru supplies oxygen species to oxidize adsorbed CO to CO<sub>2</sub>. This hypothesis strongly supports the theory that a bifunctional mechanism is active for ethanol oxidation.

Fig. 6(c) shows 2-propanol oxidation behaviour on Pt-Ru/C over the same temperature range. Four current peaks are observed on the positive potential scan. The first (a<sub>1</sub>) is at about 0.2 V, the second (a<sub>2</sub>) at about 0.6 V, the third (a<sub>3</sub>) at about 0.85 V, and fourth (a<sub>4</sub>) at about 1.1 V. The 'a<sub>1</sub>' peak is not observed with Pt/C, see Fig. 2(c), because of the Ru addition effect on 2-propanol oxidation. The 'a<sub>1</sub>' peak has been associated with a dehydrogenation process [8]. Indeed, it has been shown that Ru facilitates both C–C bond cleavage and dehydrogenation for ethanol oxidation [15]. This idea somewhat contradicts the previous work by Rodrigues et al. [8], which states that Ru has a weak effect on the shift of the onset potential for 2-propanol oxidation. Similar to 2-propanol oxidation at Pt/C, the 'a<sub>3</sub>' peak becomes dominant at higher temperatures. Also, reduction currents are observed on the negative potential scan, as has a single

re-oxidation peak, due to the strong adsorption of OH on Ru. In addition, the re-oxidation peak is very large, which indicates that a significant number of reaction intermediates is adsorbed.

2-Butanol oxidation shows a resemblance to 2-propanol oxidation, as demonstrated by Fig. 6(d). Four current peaks are observed. The first (a<sub>1</sub>) is at about 0.2 V, the second (a<sub>2</sub>) at 0.55 V, the third (a<sub>3</sub>) at about 0.9 V, and the fourth (a<sub>4</sub>) at about 1.1 V. At higher temperatures, the first and the third peaks become dominant while the second peak diminishes. Although the reduction of oxide species and re-oxidation peaks increase with temperature, the temperature effect is negligible for 2-butanol oxidation.

#### 4.2. Effect of varying the scan rate

Fig. 7(a) and (b) show CVs obtained at different scan rates at 25 and 80 °C, respectively. In Fig. 7(a), it is observed that currents at 0.5 V increase with scan rate with a simultaneous current reduction at about 0.7 V. This behaviour is similar to



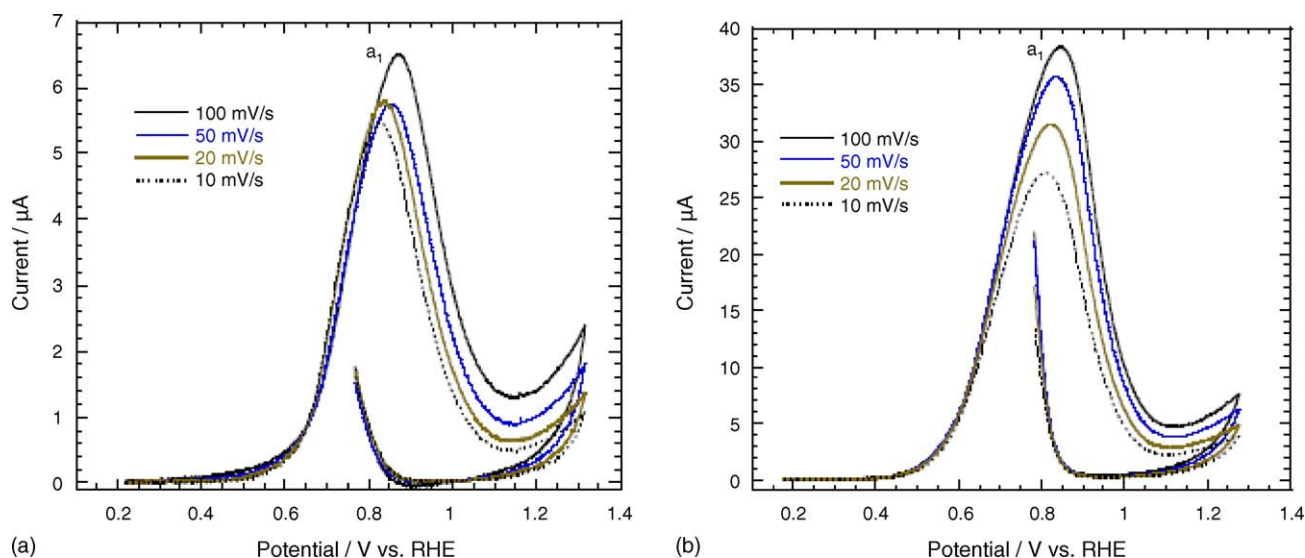


Fig. 7. Cyclic voltammograms at different scan rates with Pt–Ru/C in 0.5 M methanol + 0.5 M H<sub>2</sub>SO<sub>4</sub>, at (a) 40 °C, and (b) 80 °C.

that of methanol oxidation on Pt/C shown in Fig. 2(a), although Pt–Ru/C also gives a negligibly smaller current shoulder at about 0.7 V. A shift in peak potential is observed with increase in scan rate at 25 °C. Thus, a slow charge-transfer process prevails at this temperature. By contrast, the CVs at 80 °C, as in Fig. 7(b), have much less shift of peak potential than those at 25 °C, which indicates that methanol oxidation is much faster at higher temperatures. The consistency of onset potentials with scan rates at 80 °C is evidence of a fast reaction.

A more obvious temperature effect is observed with ethanol oxidation, as shown in Fig. 8(a) and (b). The current increase at 0.6 V with reduction of the current shoulder at 0.8 V is clearer with ethanol oxidation, see Fig. 8(a). A dependence of the potential of peak ‘a<sub>1</sub>’ on the scan rate is also observed. The CVs at 80 °C (Fig. 8b) however, show that the peak potential is unaffected by the scan rate and, moreover, there is an overlapping of the oxidation and reoxidation peak potentials. These findings

indicate that ethanol oxidation at 80 °C is a reversible charge-transfer process.

Fig. 9(a)–(d) are CVs for 2-propanol oxidation over a temperature range of 25–80 °C. Four current peaks are observed at about 0.25 V (a<sub>1</sub>), 0.65 V (a<sub>2</sub>), 0.9 V (a<sub>3</sub>), and 1.2 V (a<sub>4</sub>). The potential of the ‘a<sub>1</sub>’ peak shows a slight dependence on scan rate at 25 °C, as shown in Fig. 9(a). By contrast, the potential of the ‘a<sub>2</sub>’ peak is unaffected by the scan rate, even at 25 °C (Fig. 9a). With increasing temperature, the ‘a<sub>3</sub>’ peak becomes dominant. For example, the peak current is not influenced by the scan rate at temperatures above 60 °C, as in Fig. 9(c) and (d), which is similar to 2-propanol oxidation on Pt/C, see Fig. 4(c) and (d). The reason for this is still unknown. At higher temperatures, the potential of the first peak also becomes independent of the scan rate, as shown in Fig. 9(d). In particular, 2-propanol reports reduction currents on the negative potential scan. This is not the case for either methanol or ethanol. This suggests that

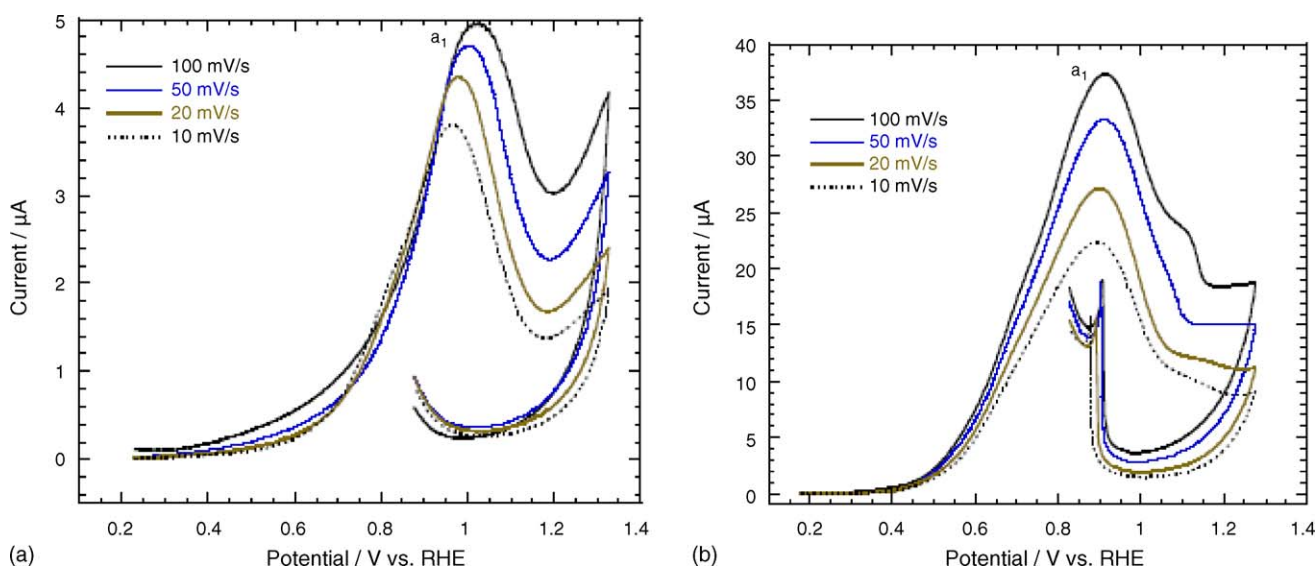


Fig. 8. Cyclic voltammograms at different scan rates with Pt–Ru/C in 0.5 M ethanol + 0.5 M H<sub>2</sub>SO<sub>4</sub>, at (a) 25 °C (a), and (b) 80 °C.

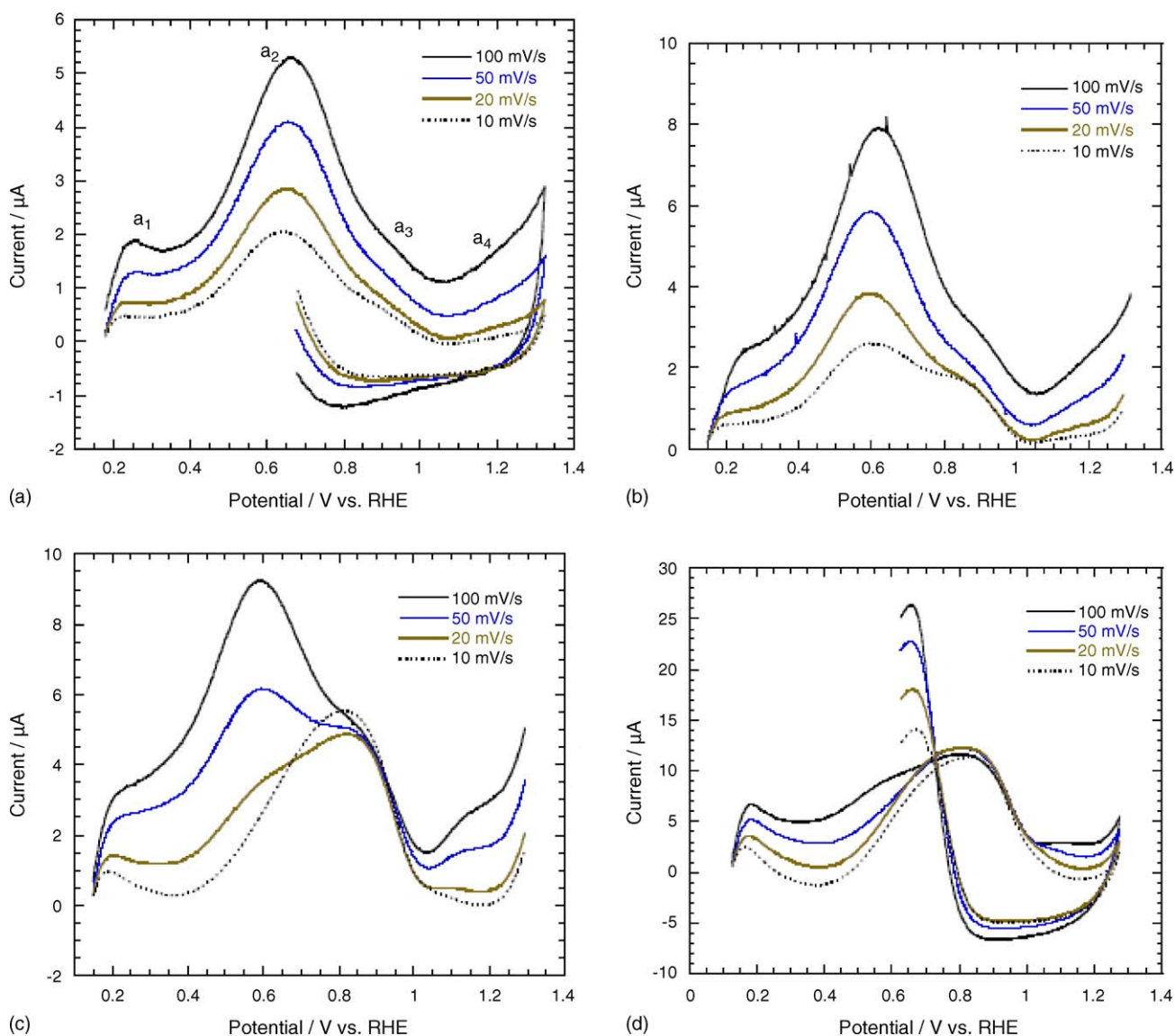


Fig. 9. Cyclic voltammograms at different scan rates with Pt–Ru/C in 0.5 M 2-propanol + 0.5 M H<sub>2</sub>SO<sub>4</sub>, at (a) 25 °C, (b) 40 °C, (c) 60 °C, (d) 80 °C.

2-propanol gives much more oxygen-containing reaction intermediates than methanol or ethanol. The reduction currents on Pt–Ru/C are much larger than those on Pt/C in Fig. 1(c). Thus, Ru in the electrocatalyst magnifies the reduction currents, i.e., Ru strongly adsorbs oxide species.

Although the oxidation currents of 2-butanol are very small compared with those of 2-propanol, there is some similarity with the CV behaviour of 2-butanol (Fig. 10(a) and (b)) and 2-propanol (Fig. 9(a)–(d)) on Pt–Ru/C. Four peaks are observed at about 0.2 V (a<sub>1</sub>), 0.55 V (a<sub>2</sub>), 0.9 V (a<sub>3</sub>), and 1.1 V (a<sub>4</sub>). The ‘a<sub>1</sub>’ peak is very small at 25 °C, but becomes dominant at 80 °C. This is probably due to a dehydrogenation process and is indicative of the fact that the oxidation of 2-butanol is facilitated at higher temperatures. The potential of ‘a<sub>2</sub>’ peak shows hardly any dependence on the scan rate, even at 25 °C as shown in Fig. 10(a). The high dependence of the ‘a<sub>2</sub>’ peak current on the scan rate indicates that the adsorption process is related to the ‘a<sub>2</sub>’ peak. On the other hand, suppressed ‘a<sub>2</sub>’ peaks and a

very weak scan rate dependence of the ‘a<sub>3</sub>’ peak are observed at 80 °C, as illustrated in Fig. 10(b). Oxidation at the ‘a<sub>3</sub>’ peak is dominant at higher temperatures, while the adsorption process of ‘a<sub>2</sub>’ becomes insignificant. This behaviour is only observed for 2-propanol and 2-butanol, despite the Ru content in the Pt based electrocatalysts. Thus, the secondary alcohols have different oxidation mechanisms at different temperatures.

Table 2 summarizes the kinetic values for the onset potential, peak potentials, peak currents, the slope of  $\log(i)/\log(v)$  and activation energies for methanol, ethanol, 2-propanol and 2-butanol oxidations on Pt–Ru/C microporous electrodes. Much lower onset potentials are observed with Pt–Ru/C than with Pt/C. In addition, the onset potential decreases for higher carbon alcohols. Ethanol shows a positive shift of about 80 mV at the ‘a<sub>1</sub>’ peak potential compared with methanol and this results in a large overpotential for ethanol oxidation. Much larger current increases are observed on Pt–Ru/C than on Pt/C for methanol and ethanol oxidations. The slopes of  $\log(i)/\log(v)$  at the ‘a<sub>3</sub>’

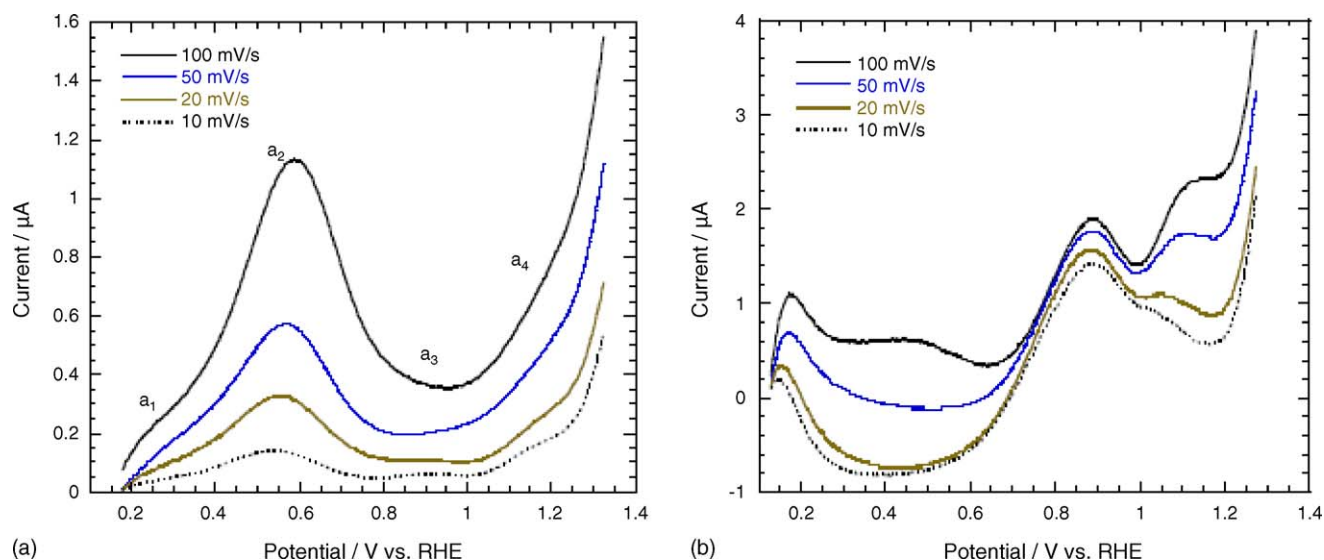


Fig. 10. Cyclic voltammograms at different scan rates with Pt–Ru/C in 0.5 M 2-butanol + 0.5 M H<sub>2</sub>SO<sub>4</sub>, at (a) 25 °C, at (b) 80 °C.

Table 2  
Kinetic values of various alcohol oxidations with Pt–Ru/C microporous electrode

Alcohols	Temperature (°C)	Onset potential (V vs. RHE)	Peak potential, $E_p$ (V at 0.1 V s <sup>-1</sup> )				Peak current, $I_p$ (µA at 0.1 V s <sup>-1</sup> )				Slope of $\log(i)/\log(v)^a$				Activation Energy/kJ mol <sup>-1</sup>				
			a <sub>1</sub>	a <sub>2</sub>	a <sub>3</sub>	a <sub>4</sub>	a <sub>1</sub>	a <sub>2</sub>	a <sub>3</sub>	a <sub>4</sub>	a <sub>1</sub>	a <sub>2</sub>	a <sub>3</sub>	a <sub>4</sub>	a <sub>1</sub>	a <sub>2</sub>	a <sub>3</sub>	a <sub>4</sub>	
Methanol	25	0.531	0.916				1.80				0.15				47.9				
	40	0.512	0.873				6.48				0.06								
	60	0.464	0.845				16.78				0.07								
	80	0.420	0.847				38.24				0.15								
Ethanol	25	0.485	1.020				4.96				0.11				30.8				
	40	0.435	0.945				13.05				0.26								
	60	0.395	0.916				20.86				0.22								
	80	0.355	0.911				37.30				0.22								
2-Propanol	25	0.179	0.254	0.663			1.89	5.28			0.60	0.41			19.3	13.0	39.3		
	40	0.150	0.257	0.618			2.42	7.92			0.59	0.48							
	60	0.145	0.218	0.591	0.840			3.23	9.26	5.22			0.53	–0.02					
	80	0.126	0.185	0.802				6.72	11.67				0.43	0.01					
2-Butanol	25	0.179	0.587				1.13				0.87				0.2	31.8	8.2		
	40	0.169	0.560				1.44				0.96								
	60	0.149	0.532	0.905	1.139			1.16	0.98	1.96			0.83	0.13					
	80	0.129	0.352	0.890	1.176	1.09			1.88	2.32			0.13	0.42					

<sup>a</sup>  $v$ : scan rate.

peaks are very low compared with the 'a<sub>1</sub>' or 'a<sub>2</sub>' peaks for the secondary alcohol oxidations. The high value of the slopes for the 'a<sub>1</sub>' and 'a<sub>2</sub>' peaks of secondary alcohol indicates that adsorption is associated with the oxidation processes. The activation energies of the 'a<sub>3</sub>' peaks are close to those of methanol and ethanol oxidation. Oxidation processes similar to methanol and ethanol occur during the oxidation of the secondary alcohols at higher temperatures.

## 5. Conclusions

From the cyclic voltammetric analysis of methanol, ethanol, 2-propanol and 2-butanol oxidations with Pt/C and Pt–Ru/C microporous electrodes, the following conclusions are drawn.

- (1) Methanol exhibits the highest increase in oxidation current with temperature, regardless of the electrode material.
- (2) For the secondary alcohols, the peak potentials are invariable with respect to the scan rate, which is probably due to the lack of accompanying C–C bond breaking.
- (3) The secondary alcohols show complicated current behaviour with temperature and, moreover, of the current peaks are unaffected by a change in scan rate at higher temperatures. These observations indicate that the secondary alcohols are oxidized by different reaction mechanisms at higher temperatures.
- (4) The effects of Pt and Pt–Ru on the oxidation of alcohols are obvious. Ru addition results in a negative shift of the onset

potential for all alcohols. In addition, Ru provides oxidation currents at about 0.2 V, probably due to dehydrogenation of 2-propanol and 2-butanol.

- (5) The strong adsorptivity of oxide species on Ru results in different oxidation and re-oxidation current peaks on positive and negative potential scans, respectively.
- (6) The microporous electrode used for catalyst evaluation has no binder and this allows more precise kinetic information on alcohol oxidation to be obtained.

## References

- [1] A. Kabbabi, R. Faure, R. Durand, B. Beden, F. Hahn, J.-M. Leger, C. Lamy, *J. Electroanal. Chem.* 444 (1998) 41–53.
- [2] A. Hamnett, *Catal. Today* 38 (1997) 445–457.
- [3] G.T. Burstein, C.J. Barnett, A.R. Kucernak, K.R. Williams, *Catal. Today* 38 (1997) 425–437.
- [4] V.M. Schmidt, R. Ianniello, E. Pastor, S. Gonzalez, *J. Phys. Chem.* 10 (1996) 17901–17908.
- [5] H. Hitmi, E.M. Belgsir, J.-M. Leger, C. Lamy, R.O. Lenza, *Electrochim. Acta* 39 (1994) 407–415.
- [6] Z. Qi, M. Hollett, A. Attia, A. Kaufman, *Electrochem. Solid-State Lett.* 5 (2002) A129–A130.
- [7] D. Cao, S.H. Bergens, *J. Power Sources* 124 (2003) 12–17.
- [8] I.A. Rodrigues, J.P. de Souza, E. Pastor, F.C. Nart, *Langmuir* 13 (1997) 6829–6835.
- [9] D. Takky, B. Beden, J.-M. Leger, C. Lamy, *J. Electroanal. Chem.* 193 (1985) 159–173.
- [10] E. Pastor, S. Gonzalez, A.J. Arvia, *J. Electroanal. Chem.* 395 (1995) 233–242.
- [11] S.-G. Sun, Y. Lin, *Electrochim. Acta* 41 (1996) 693–700.
- [12] D. Takky, B. Beden, J.-M. Leger, C. Lamy, *J. Electroanal. Chem.* 145 (1983) 461–466.
- [13] D. Takky, B. Beden, J.-M. Leger, C. Lamy, *J. Electroanal. Chem.* 256 (1988) 127–136.
- [14] M. Watanabe, S. Motoo, *J. Electroanal. Chem.* 60 (1975) 267–273.
- [15] R. Ianniello, V.M. Schmidt, J.L. Rodriguez, E. Pastor, *J. Electroanal. Chem.* 471 (1999) 167–179.
- [16] N. Fujiwara, K.A. Friedrich, U. Stimming, *J. Electroanal. Chem.* 472 (1999) 120–125.
- [17] A.V. Tripkovic, K.D. Popovic, B.N. Grgur, B. Blizanac, P.N. Ross, N.M. Markovic, *Electrochim. Acta* 47 (2002) 3707–3714.
- [18] D. Kardash, C. Korzeniewski, N. Markovic, *J. Electroanal. Chem.* 500 (2001) 518–523.
- [19] C.-G. Lee, T. Itoh, M. Mohamedi, M. Umeda, I. Uchida, H.-C. Lim, *Electrochemistry* 71 (2003) 549–554.
- [20] E. Ticanelli, J.G. Beery, M.T. Paffet, S. Gottesfeld, *J. Electroanal. Chem.* 258 (1989) 61–77.
- [21] A.J. Bard, L.R. Faulkner, *Electrochemical Methods*, John Wiley & Sons, 2001, pp. 226–243.
- [22] H. Wang, C. Wingender, H. Baltruschat, M. Lopez, M.T. Reets, *J. Electroanal. Chem.* 509 (2001) 163–169.
- [23] H.A. Gasteiger, N. Markovic, P.N. Ross Jr., E.J. Cairns, *Electrochim. Acta* 39 (1994) 1825–1832.